Journal of Materials Research and Technology 40 (2026) 3422–3435

Contents lists available at ScienceDirect

Journal of Materials Research and Technology

journal homepage: www.elsevier.com/locate/jmrt

Mechanical and microstructural characterization of graphene dispersed basalt fiber reinforced polymeric composites

G. Karthikeyan [a], Rajini Nagarajan [a,*], Sikiru O. Ismail [b], Faruq Mohammad [c], Kumar Krishnan [d], M.P. Indira Devi [e]

[a] Department of Mechanical Engineering, Kalasalingam Academy of Research and Education, Krishnankoil, 626126, India
[b] Centre for Engineering Research, School of Physics, Engineering and Computer Science, University of Hertfordshire, Hatfield, Hertfordshire, AL10 9AB, United Kingdom
[c] Department of Chemistry, College of Science, King Saud University, P.O. Box 2455, Riyadh, 11451, Kingdom of Saudi Arabia
[d] INTI International University, Persiaran Perdana BBN, 71800, Nilai, Negeri Sembilan, Malaysia
[e] Department of Physics, Ramco Institute of Technology, Rajapalayam, 626117, India

ARTICLE INFO

Keywords:
Mechanical properties
Microstructural behaviors
Characterization
Graphene
Basalt fiber
Product innovation

ABSTRACT

This study focused on effects of graphene nanofiller on basalt/epoxy composites. Basalt epoxy (BE) composite samples were fabricated by dispersing graphene in n-Butanol, using hand layup method. Fabricated materials were subjected to mechanical (tensile, flexural and impact) testing according to the ASTM standards. Interfacial characterization, failure morphology and internal structure of the fractured surfaces of the tested samples were carried out, using scanning electron microscope (SEM). From the results obtained, it was observed that addition of graphene nanofiller notably enhanced the mechanical properties: tensile strength and modulus, flexural and impact strengths of the composite samples. Graphene imposed composite, designated as basalt/epoxy-graphene (BEG) sample recorded 9.98 % higher tensile strength than BE counterpart. Similarly, its flexural and impact strengths increased by 58.34 % and 97.30 %, respectively. These can be attributed to presence of graphene nanofiller in basalt/epoxy composite system. Considering further study on their microstructures, it was observed that graphene enhanced the interfacial adhesion bonding between basalt fiber and epoxy matrix, which consequently improved the mechanical properties of the BEG composites. This investigation can inform better design, fabrication and application of fiber reinforced polymeric composites.

1. Introduction

The development of composite materials, which are extensively utilized in the automotive, engineering and aerospace industries, is greatly influenced by the growing demand for a wide range of materials. Because of their superior mechanical qualities, such as stiffness, flexibility and modulus, natural fibers have played a significant role in the evolution of composites to meet the demand of several sectors. Due of their affordability, accessibility, and environmentally beneficial qualities, these materials are widely used.

Composite material in general is a combination of fiber and polymer, which are known as reinforcement and binder, acting as load bearing and transferring components, respectively. Many composite materials are replacing the conventional materials by enhancing the basic properties of natural fibers, using various improved types of fibers, matrices, fabrication methods and other constituent materials. Apart from matrix and reinforcement, there are nanofillers which can be used alone or in combination. Examples include, but are not limited to, graphene, carbon nano tubes, nano clay and ceramics, as subsequently elucidated.

Nanomaterials are increasingly utilized in polymer composites to enhance mechanical, thermal, electrical and optical performance, due to their high surface area and unique physicochemical properties, enabling synergistic effects beyond conventional reinforcements. Typical nanofillers include silicon dioxide or silica (SiO_2), aluminum oxide or alumina (Al_2O_3), zinc oxide (ZnO), titanium dioxide (TiO_2), graphene, graphene oxide and multi-walled carbon nanotubes (MWCNTs), selected according to the targeted application and property enhancement. These nanofillers are combined with fibers, derived from natural sources, such as coir, kenaf, hemp, jute, flax, bamboo and sisal or synthetically produced, including E-glass, aramid and carbon fibers, acting as the primary load-bearing constituents. Their choice depends on the polymer matrix, processing technique and end-use requirements, with fabrication

* Corresponding author.
E-mail address: rajiniklu@gmail.com (R. Nagarajan).

https://doi.org/10.1016/j.jmrt.2025.12.235
Received 29 October 2025; Received in revised form 22 December 2025; Accepted 22 December 2025
Available online 24 December 2025

methods: filament winding, spray-up, injection moulding, compression moulding and additive manufacturing, among others. Increasing environmental and health concerns have driven a shift toward natural fibers, as sustainable alternatives to synthetic fibers. Furthermore, hybrid fiber/nanomaterial reinforced composites provide superior multifunctional properties when nanomaterials are uniformly dispersed in the matrix, ensuring efficient load transfer at the fiber–matrix interface, though excessive filler loading may induce brittleness and limit tensile performance.

Epoxy resins are reactive polymers that cure through a hardener, forming strong, durable and chemically resistant materials that are widely used in construction, automotive, electronics and coatings, due to their strength, adhesion and reliability. Graphene, available in forms, such as pristine graphene, graphene oxide (GO) and reduced graphene oxide (rGO), enhances polymer composites by improving strength, conductivity, dispersibility and thermal stability, while advanced forms such as graphene nanoplatelets, nanoribbons, quantum dots and aerogels enable tailored applications in sensors, coatings, energy storage and heat dissipation. Basalt fiber, a natural, biodegradable and corrosion-resistant reinforcement derived from basalt rock, offers superior strength, reduced weight and design flexibility. It is produced by melting volcanic rock at 1400–1700 °C and extruding filaments, basalt fibers gain enhanced adhesion through surface coating and have become a sustainable alternative to synthetic fibers, finding increasing use in modern engineering applications. Many studies have been reported to establish basalt fiber as a good reinforcement for composite structures. Most relevant findings to this research are subsequently discussed.

Pradeep et al. [1] investigated basalt fiber reinforced composites fabricated by hand layup method and subjected to mechanical testing, hardness and wear study according to ASTM standards. They observed that SiO_2 nano fillers significantly improved the flexural properties of the composites, The addition of SiO_2 nanofiller nanoparticles enhanced the hardness of the composite by reinforcing the polymer matrix, resulting in a more compact and dense structure, and the wear resistance improved, owing to the better interfacial bonding and reduced wear debris size. Kumar et al. [2] reported that hybrid composites had a better tensile strength than the untreated coconut sheath fiber (UTCSF) composite), although it was lower than that of the pristine basalt fiber composite, owing to the high stiffness of the basalt fiber. The high tensile strength of the basalt fibers contributed to the high tensile strength of the hybrid composites. The incorporation of basalt fibers, known for their stiffness, significantly improved all the properties in the hybrid composites. Ankit et al. [3] compared the mechanical properties of epoxy, with reinforcements of E-glass, aramid and carbon fibers in their composites fabricated by hand layup method. It was observed that Kevlar reinforcing composite produced the highest flexural strength. The tensile strength of the Kevlar composite was the best among the test samples at 51.42 MPa, representing a 56 % improvement over the epoxy neat. Kevlar recorded a very high elongation of 13.67 %.

Furthermore, Totara et al. [4] compared glass fiber (GF) and basalt fiber reinforced composites (BFRC), using vinyl ester as matrix. The mechanical properties and failure mechanisms of BFRC and GFRC were analyzed and compared under static tensile tests. Distinct fiber failure mechanisms were observed. BF components continued to bear the load, allowing the component to survive longer without catastrophic breakage. BFRC exhibited a progressive failure, with initial fibers breakage, followed by delamination and debonding mechanisms until the sample failed. GFRC experienced sudden and complete failure, with strong inter-laminar bonding and there was no layer delamination observed. Kabir et al. [5] investigated effect of incorporation of cow bone at various proportions as a filler, using epoxy as a matrix and glass fiber as a reinforcement. Tensile strength increased by adding cow bone powder and it was observed that it enhanced the bonding of matrix and reinforced material. There was a gradual decrease of flexural strength with an increasing filler content. This can be associated with stress concentration in where filler particles acted as stress concentrators, leading to localized high stress areas that initiated failure at lower loads. Poor interfacial adhesion: bonding between filler and matrix was weak, load transfer was inefficient, reducing overall strength and creating weak points in the material. Impact strength increased with low amount of filler content. This was due to improved stress distribution, interfacial adhesion, particle size and distribution.

Anandh et al. [6] examined the mechanical properties, water absorption capacity, fatigue strength and microstructural characteristics of a hybrid composite reinforced with basalt and Kevlar fibers and porcelain fillers. It was observed that the dominance of Kevlar in the sequence was likely responsible for the superior performance under impact, as Kevlar was known for its excellent energy absorption and toughness. The moderate filler content cause an optimal balance between matrix stiffness and flexibility, allowing the composite to absorb and dissipate impact energy effectively without becoming overly brittle. Velumayil and Palanivel [7]. studied Kevlar/epoxy, basalt/epoxy and hybrid laminates via hand layup and observed that the hybrid showed the highest tensile strength. Also, scanning electron microscope (SEM) revealed good matrix bonding, fiber deflection under bending and resilience of basalt under load. Impact strength was highest for basalt/Kevlar/epoxy hybrids, followed by Kevlar/basalt/epoxy. Generally, hybrid properties dropped between pure laminates, though some exceeded them, indicating potential of hybridization and the need for further study.

Xiao-Hui et al. [8] evaluated the influence of novel piperazine phosphonate flame retardant on epoxy–basalt composites fabricated by hand layup method. The observations implied the crack deflection during the propagation of cracks, leading to the absorption and dissipation of impact energy throughout the fracturing process. Consequently, epoxy/piperazine phosphonate flame retardant (EP/PDIP) and basalt fiber (BF)/EP/PDIP) demonstrated superior impacted strength. The secondary amine groups present in PDIP reacted with epoxy groups, while its rigid phenyl structure enhanced the stiffness of the resulting composite matrix. This contributed to the improved flexural strength and interlayer shear strength of the samples. Palaniyandia and Veeman [9] fabricated basalt fiber reinforced composites through pressure mould by incorporating carbon nanotubes and nanosilicon carbide particles. They observed that effective matrix-reinforcement interfacial bonding and homogeneous diffusion of SiC/MWCNT fillers into the matrix resulted in an improvement in tensile strength. The flexural strength was significantly higher for pristine composites. The improved interfacial bonding of matrix and reinforcing material caused higher tensile strength.

Besides, studies have been extended to basalt fiber reinforced polymer composites filled with nanofillers, as subsequently reported. Khosravi and Reza [10] studied basalt fiber/epoxy composites modified with 3-glycidyloxypropyltrimethoxysilane (3-GPTS)/Na-montmorillonite (Na–Mt) nanoclay (0–5 wt%). Incorporation of 5 wt% nanoclay enhanced tensile strength and modulus by 11 and 23 %, flexural strength and modulus by 28 %, and compressive strength and modulus by 43 and 34 %, respectively. While unfilled composites exhibited fiber–matrix debonding, nanoclay addition markedly improved interfacial adhesion and induced crack deflection. Wang et al. [11] manufactured basalt fiber/phenolic resin composites incorporating SiO_2 and graphite (<1 μm) nanofillers. The hybrid basalt fiber/graphene/silicon oxide (BF/Gr/SiO_2) composite exhibited 58.5 % higher friction coefficient and significantly reduced wear rate under high loads when compared with the unfilled basalt fiber composite (BFC). While pristine BFC exhibited fiber pull-out and matrix–fiber debonding, filler addition minimized fiber pull-out and breakage. Tribological performance was further enhanced by a thin wear debris layer, which acted as a lubricant, preventing direct contact between the composite and its counterpart. Bahari-Samtan et al. [12] investigated epoxy composites reinforced with basalt fiber, 0.5 mm aluminium sheets and unmodified or surface-modified nanoclay (0–5 wt%). Flexural and impact strengths increased with nanoclay content, with 3 wt% modified nanoclay

composites exhibiting 52 and 10 % improvements, respectively, over the control. Composites containing modified nanoclay outperformed than those with unmodified nanoclay, as reduced agglomeration minimized brittleness and enhanced overall mechanical performance.

Vinay et al. [13] examined basalt fiber/epoxy composites reinforced with α-nano alumina (0–3 wt%). Tensile strength decreased with filler addition, whereas 0.4 wt% composites exhibited a 31 % increase in flexural strength, and 0.6 wt% composites showed 23 % higher interlaminar shear strength (ILSS) when compared with the unfilled samples. Wear rate decreased and hardness increased with filler content. Property enhancement at low filler content was attributed to uniform filler dispersion, while higher loadings induced agglomeration, interfacial debonding, fiber pull-out and breakage. Arshad et al. [14] investigated bio- and synthetic epoxy composites reinforced with coconut and basalt fibers, coconut micro-particles and titanium carbide (TiC) nanoparticles. Addition of TiC nanoparticles roughened the composite surface, while failures were primarily caused by small gaps and non-uniform fiber and filler dispersion. Subagia et al. [15] fabricated epoxy composites reinforced with woven basalt fiber and tourmaline powder (900 nm–8 μm) at 0.5–2 wt%. Both flexural strength and modulus increased with filler content, over unfilled basalt fiber reinforced polymer (BFRP). Improved matrix–fiber bonding and uniform dispersion of tourmaline particles contributed to strong interfacial adhesion.

In addition, Chen et al. [16] studied epoxy composites reinforced with unidirectional basalt fiber and graphene nano platelets (GnPs) which exhibited enhanced mechanical properties, with maximum strength and modulus achieved at 0.07 wt% GnPs in hybrid composites. At low filler loadings, GnPs were uniformly dispersed, while higher loadings led to agglomeration and conductive network formation, reducing property gains. Gulut [17] reported basalt plain fabric/epoxy composites reinforced with graphene nanoplatelets (0–0.3 wt%). At 0.1 wt% GnPs, tensile strength and modulus increased by 13 and 19 %, flexural strength and modulus by 30 and 69 % respectively, and impact strength by over 11 %. Higher filler loadings led to property deterioration, due to agglomeration, fiber pull-out and interfacial debonding. Lee et al. [18] investigated epoxy composites reinforced with woven basalt fiber and unmodified, oxidized and silanized CNTs. Silanized CNT/basalt/epoxy composites exhibited 60 % higher Young's modulus and 34 % higher tensile strength than unmodified counterparts, along with a 48 % increase in storage modulus, due to strong cross-linked networks, uniform CNT dispersion and enhanced matrix–CNT interfacial adhesion. Improved interfacial bonding reduced matrix mobility, enhancing thermal stability. Fracture analysis revealed significant fiber pull-out and CNT agglomeration in unmodified composites, reduced pull-out in oxidized composites and minimal fiber pull-out with well-dispersed CNTs in silanized composites.

Kim et al. [19] developed epoxy composites reinforced with basalt fiber (plain weave) coated with MWCNTs via cyclic dip–dry coating (0–10 cycles). Flexural strength and modulus increased with coating cycles. Further cycles reduced properties, due to MWCNT agglomeration and impaired load transfer. MWCNTs adhered tightly through hydrophobic interactions and specific bonding, producing a progressively rougher fiber surface with increasing coating cycles. Similarly, Kim et al. [20] studied epoxy composites reinforced with woven basalt fiber and MWCNTs treated with acid or silane. Silane-modified CNT/basalt/epoxy composites exhibited higher flexural strength, modulus and greater fracture toughness than acid-treated counterparts. These results were attributed to improved CNT dispersibility and interfacial adhesion, enabling uniform load transfer. Fracture analysis revealed reduced fiber pull-out and enhanced matrix–fiber bonding in silanized composites. Chen et al. [21] investigated basalt fiber/epoxy composites reinforced with MWCNTs (0–1.5 vol%). The research reported that surface-modified CNTs improved interfacial stress transfer via covalent bonding and uniform dispersion, while promoting toughening mechanisms, such as crack deflection, fracture pinning and reduced fiber–matrix debonding.

Several studies have addressed basalt fabric reinforced polymer composites for various applications, due to their less impact on environmental hazards constituencies. Huanag et al. [22] proposed a nacre-inspired biomimetic laminate architecture to enhance the impact resistance of basalt fiber–reinforced polymer (BFRP) composites. Through low-velocity impact testing and ultrasonic C-scan evaluations, supported by meso–macro finite element modeling, the study demonstrated that a misaligned, nacre-like structural design effectively restricted crack propagation and promoted tortuous energy-dissipation pathways. This work highlighted the significance of tailored microstructural arrangements in improving the damage tolerance of BFRP laminates. Recent developments in multifunctional BFRP systems further emphasised the potential of integrating functional phases to achieve *in-situ* damage of self-sensing and temperature-responsive behavior. These advancements collectively underlined the growing research interest in enhancing the mechanical performance and functional capabilities of basalt fiber composites, providing a strong motivation to investigate graphene-based dispersion strategies for improving the structural and microstructural characteristics of BFRP composites. Zheng et al. [23] examined the seawater corrosion behavior of basalt/epoxy composites enhanced with KH560 and carboxylated CNTs. Their results showed that the modified system exhibited markedly improved retention of flexural strength, modulus and interlaminar shear strength during long-term exposure, owing to an improved multiscale stress-transfer interface. Even after extended ageing at elevated temperature, the modified composites suffered substantially lower property degradation than the unmodified counterparts, highlighting the effectiveness of nanoscale interfacial modification in improving the durability of BFRP materials for marine environments. Liu et al. [24] introduced a multifunctional BFRP system by creating a CNT-surrounding-basalt (CSB) architecture via electrostatic self-assembly and melt mixing. This engineered microstructure enabled a low electrical percolation threshold, enhanced conductivity and improved mechanical properties. The resulting composites exhibited reliable damage self-sensing and notable temperature-responsive behavior, highlighting the potential of nanoscale hybridization strategies for developing next-generation sensing-enabled BFRP materials.

Recent work [25] by other researchers has explored multi-scale reinforcement strategies to improve the performance of basalt fiber–reinforced epoxy composites. The study developed epoxy laminates reinforced with KH560-modified basalt fibers and carboxylated CNTs, achieving a strong BF/CNT interface through surface grafting and impregnation. FTIR, XPS, and SEM analyses confirmed successful chemical modification and improved resin–fiber adhesion. The optimal KH560 content at 5 % resulted in notable improvements in tensile, flexural and interlaminar shear properties, due to more efficient load transfer at the interface. Additionally, the modified composite exhibited enhanced thermal stability, with increases in both the decomposition onset temperature and residual mass. These findings demonstrated the effectiveness of combined silane treatment and CNT hybridization in strengthening the mechanical and thermal behaviors of BFRP systems. Furthermore, studies have also examined the environmental durability of fiber-reinforced polymer composites under extreme service conditions. The research evaluated raw fibers and unidirectional FRPs in high-temperature, high-pressure H_2S/CO_2 environments, representative of oil and gas field conditions. It was reported that basalt fibers exhibited significantly better degradation resistance than glass fibers. BFRP composites produced comparatively lower reductions in flexural modulus, flexural strength and interlaminar shear strength, while GFRP experienced severe property losses and extensive cohesive interface damage. Finite element method (FEM) used further confirmed that BFRP retained its primary failure mode, whereas GFRP exhibited pronounced interfacial degradation. These results highlighted the superior resilience of basalt fiber–based composites for demanding industrial applications [26].

Basalt fiber-reinforced polymer (BFRP) composites are increasingly

explored as a cost-effective and sustainable alternative to glass and carbon fiber composites, due to their excellent strength-to-cost ratio, high thermal stability and corrosion resistance. However, the full mechanical potential of BFRPs is often limited by insufficient interfacial adhesion between the chemically inert basalt fibers and the epoxy matrix, leading to sub-optimal stress transfer and reduced damage tolerance. Meanwhile, graphene-based nanomaterials (graphene nanoplatelets, graphene oxide, among others) exhibit exceptional stiffness, large specific surface area and compatibility with surface functionalization, making them one of the most promising candidates for engineering the micro–nano interphase in structural composites.

The proposed research introduced a multiscale reinforcement strategy integrating nanoscale graphene fillers into the mesoscale basalt-epoxy framework. This combination remains relatively unexplored when compared with conventional carbon/glass composites, and it enables a unique approach to simultaneously enhance stiffness, strength and toughness. Based on the aforestated extensive literature studied, there is a research gap in achieving uniform dispersion of nanofiller in epoxy matrix. More importantly, investigation into effects of graphene nanofiller on both interrelated mechanical and microstructural behaviors of basalt fiber reinforced epoxy composites is required to advance and contribute to the composite technology, as a main objective of this study.

2. Materials and methods

2.1. Materials used

Plain fabric for composite applications was entirely made of 100 % basalt continuous filament (BCF) roving. Silane sizing was selected, which had components to ensure elasticity of the yarn during textile processes. The silane sizing allowed good compatibility with epoxy. Table 1 presents the physical properties of the basalt fiber used.

Liquid epoxy resin unmodified Epichlorydin and Bisphenol A, known as Araldite LY556 was purchased from Herenba Instruments and Engineers, Chennai. It was used as a matrix material. Table 2 presents the properties of the epoxy resin LY556.

Graphene is a two-dimensional (2D) crystalline allotrope of carbon, consisting of atoms arranged in a hexagonal lattice with sp^2 hybridization. It exhibits an exceptional optical transparency of approximately 96.6 %, combined with remarkable electrical conductivity. It records high thermal conductivity at room temperature, making it highly attractive for diverse scientific and technological applications. In this work, functionalized graphene oxide (FGO) was synthesized from graphite powder through a two-step process: (a) preparation of graphite oxide using the Hummers' method [27], and (b) subsequent functionalization to obtain FGO, following the procedure reported in previous studies [28,29]. The detailed methodology and background information on the graphene preparation processes have already been comprehensively described [30].

2.2. Fabrication of composite structure

A mould of 300 × 200 mm was first prepared. A hand layup method was employed to fabricate sample with cross-section of 300 × 200 mm (Fig. 1), as one of the oldest methods. Basalt fiber of required dimensions was obtained and laid one over another with proper orientation. Graphene of 0.1 gms was weighed accurately and mixed with butanol of 40 gms to attain uniform dispersion by placing graphene butanol solution in ultrasonicator for 2 h. An overhead projector (OHP) sheet was laid on the top of the mould for easy removal of the cured sample. The graphene butanol solution was poured in the epoxy matrix, called Araldite LY55. It weighed 100 gms and dispersed evenly using ultrasonicator for 6 h. Hardener, known as Aradur grade HY951 was weighed and poured in epoxy graphene mixture. During processing, the butanol solvent evaporated. Finally, 0.15 wt% of graphene was incorporated into the basalt fabric for the composite preparation. After preparing the graphene–epoxy solution, the basalt fabric layers were stacked sequentially, with each layer coated uniformly using the solution. The stacked laminate was then covered with an OHP sheet to achieve a smooth surface finish and left undisturbed to cure for 48 h. After the optimal curing period, the composite was removed from the mould, and the edges were trimmed to obtain the final specimen dimensions.

Table 1
Physical properties of basalt fiber used [1].

Properties	Values	Units
Density	2.65	g/cm^3
Tensile strength	4.80	GPa
Modulus of elasticity	110	GPa
Elongation percentage	3.10	%
Poisson's ratio	0.20	–

Table 2
Properties of epoxy (LY556) used (as extracted from Manufacturer Product Data).

Properties	Values	Units
Density	1.19	g/cm^3
Glass transition temperature	67	°C
Tensile strength	52	MPa
Viscosity	10350–12000	cP
Specific gravity at 25 °C	1.1–1.2	g/cm^3
Flash point	160	°C

3. Mechanical characterization of the composite samples

3.1. Tensile test

Mechanical property in terms of tensile strength was determined, using tensile testing machine with a load cell and a digital encoder, produced by the Sensotech technologies and Grayhill, respectively. Three rectangular samples of cross-section of 165 × 19 × 3 mm with gauge length of 150 mm (ASTM D638-03) were cut from the parent laminate plate (Fig. 2a). Strips were mounted on the grip and load was applied until rupture occurred. The ultimate tensile strength of the sample was determined and maximum load at failure was recorded (Fig. 2b).

Mechanical characterizations were carried out on the basalt fiber reinforced polymer composite samples to evaluate their tensile properties, including tensile strengths, Young's moduli and fracture elongations. Each measurement was repeated three times, and the average values were considered for the analysis.

3.2. Three-point bending test

Flexural strength was determined, using a similar machine. Three rectangular samples (Fig. 3a) with cross-section of 100.0 × 12.5 × 3.0 mm each and ASTM D790 standard was followed. Strips were mounted on the grip as a beam and a point load was applied at the middle of the sample (Fig. 3b). Load was applied to the sample until failure occurred. Following the test, the recorded load deflection data was converted into stress-strain curves. Flexural strength (MPa) was calculated using the formula $3FL/2bd^2$, where F, L, b and d represent load applied, sample length, breadth (or width) and depth (or thickness), respectively.

3.3. Impact test

Impact strength of the sample was determined using impact testing machine, which has load cell and a digital encoder produced by Sensotech technologies and Grayhill, respectively. Three rectangular samples (Fig. 4a) with a cross-section of 65.5 × 12.7 mm each and a notch

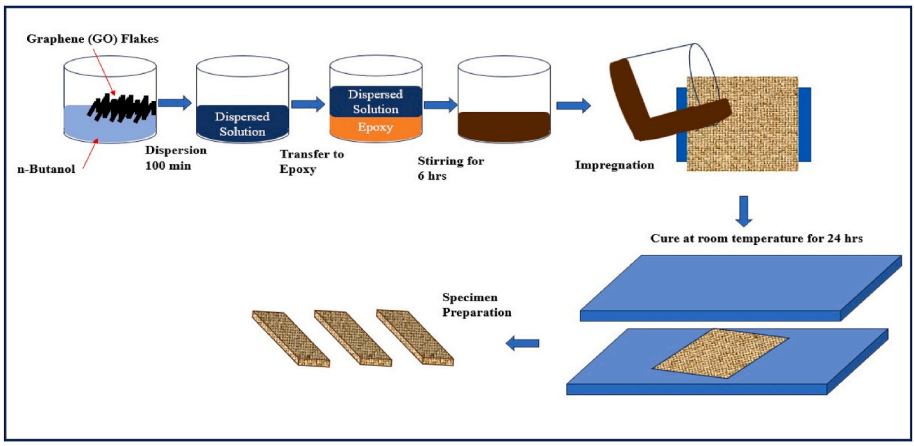

Fig. 1. Schematic diagram of fabrication process of graphene impregnated basalt fabric composite specimens.

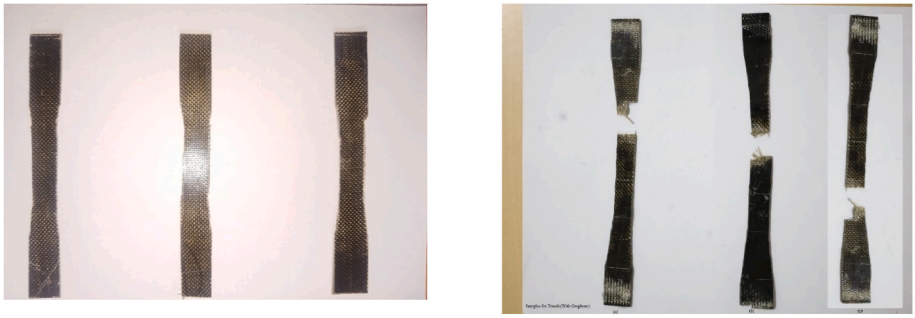

Fig. 2. Samples (a) before and (b) after tensile test.

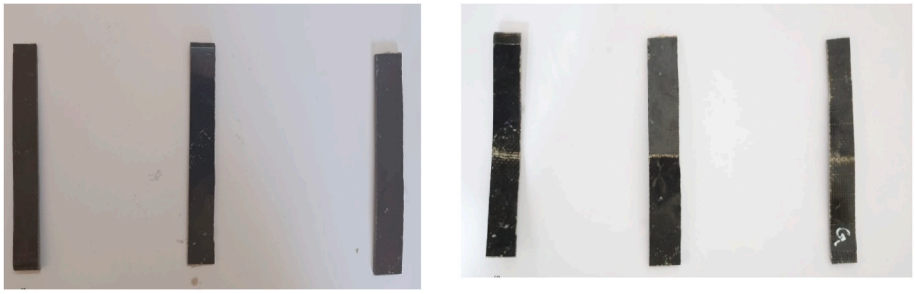

Fig. 3. Samples (a) before and (b) after three-point bending test.

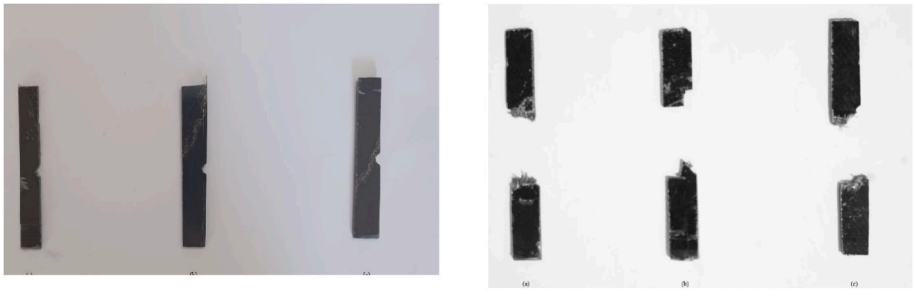

Fig. 4. Samples (a) before and (b) after impact test.

angle of 45°. ASTM D256 (Izod) standard was considered. Strips were mounted on the grip and hammer was released from the holder, which stroke or impacted the sample (Fig. 4b) and load absorption was determined. All the tests were conducted at the METMECH Analytical Engineers' Research Laboratory, located in Chennai.

4. Results and discussion

SEM micrographs with EDX were obtained to evidence the inclusion of FGO in the epoxy matrix, as shown in Fig. 5. The pure epoxy and the graphene filled epoxy showed the presence of carbon and oxygen content in EDX results. Furthermore, an increased carbon content was observed after the inclusion of graphene in epoxy matrix, which established the presence of FGO dispersion. Similar observation was also noted in previous study [31], where EDX spectrum detected a strong presence of carbon (C) as expected, due to the polymeric nature of polyvinyl acetate (PVAc) and the incorporation of GO. This high carbon content confirmed the dominant organic matrix and the effective inclusion of GO in the composite to confirm this result.

4.1. Tensile characteristics

The samples S1, S2 and S3 have been cut and tested according to the relevant ASTM standards. Mechanical strengths of the samples were considered, including tensile, flexural and impact, as subsequently elucidated in detail. Fig. 6(a) and (b) show the tensile strengths and moduli of the samples, respectively. It was evident from the results obtained that incorporation of graphene nanofiller recorded significant impact on tensile strength of the sample; the graphene-based composite sample exhibited 9.98 % increase in tensile strength.

In addition, the tensile strength of the basalt epoxy-graphene (BEG) composite sample was measured to be 238.30 MPa, which was higher than 195.79 MPa of BE counterpart. Both tensile strength and modulus of BEG sample were greater than that of BE sample. Therefore, the significance of the presence of graphene was evident. Considering tensile modulus (Fig. 6b), BEG sample showed an increment of 37 % when compared with BE sample. Besides, Table 3 presents percentage elongations of the samples. It was observed that BE samples recorded maximum or higher deformation before irreversible damage occurred when compared with BEG. This can be attributed to greater quantity of epoxy resin present in the BE samples, which could have supported more elongation before fracture.

Fig. 7(a) and (b) depict stress-strain behavior of BEG sample and Fig. 7(c) and (d) show stress-strain response of BE counterpart. From the results obtained, it was evident that all the investigated samples recorded strong elongation characteristics, because basalt fiber is known with good ductile property.

4.2. Flexural characteristics

Fig. 8 depicts the flexural strengths of the two different composite samples in form of bar chart. The flexural strengths of BEG samples S1, S2 and S3 were 376.19, 368.13 and 405.70 MPa, which were greater than BE samples with 282.99, 233.22 and 210.07 MPa, respectively. In comparison, BEG (composite with graphene content) exhibited better flexural strength of 58.34 % higher than pristine BE composite sample. Graphene was completely distributed in epoxy matrix. There was a strong interfacial interaction between fiber and matrix, because of graphene imposition. This was due to formation of chemical bonds between functional groups on graphene and matrix during curing, creating more stable interface between layers. Similarly, Sun et al. [32] reported the improved mechanical and self-sensing capabilities of BFRP laminates by modifying basalt fabrics with COOH-CNTs via electrophoretic deposition. The optimized laminate (EPD20-BFRP) achieved significant increases in both tensile and flexural moduli, due to the surface energy changes and adhesion between the fiber and matrix.

4.3. Impact characteristics

To analyze the impact strengths of the samples, experimentation was

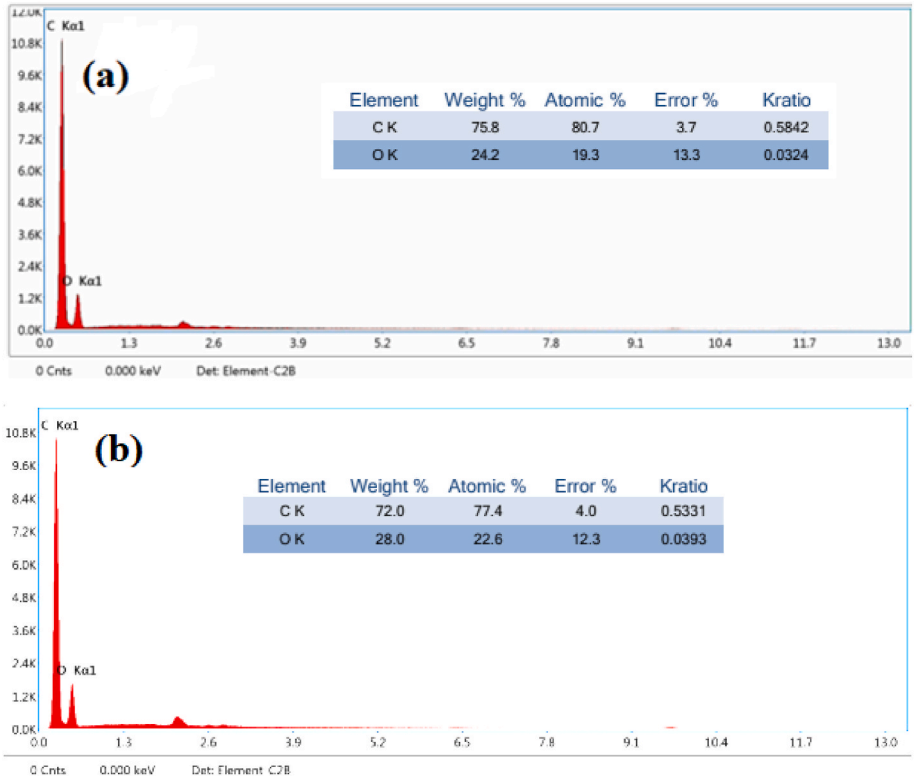

Fig. 5. EDXs of (a) BEG and (b) BE samples.

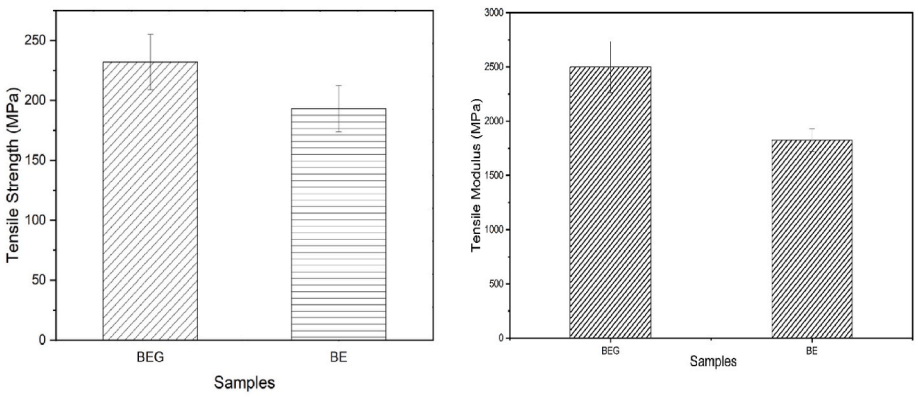

Fig. 6. Tensile (a) strengths and (b) moduli of the samples.

Table 3
Measured percentage of elongation.

% elongation		
Sample	BEG	BE
S1	7.12	12.68
S2	8.40	12.68
S3	8.40	12.68

done using impact testing machine model XJJU-5.5. Fig. 9shows the energy absorption of the two samples. Based on the results obtained, it was observed that impact strength of BEG samples S1, S2 and S3 were 10.5, 15.9 and 13.2 kJ/m^2 respectively, which were higher than BE counterpart with 7.2, 5.4 and 7.5 kJ/m^2, respectively. Therefore, BEG sample with graphene reinforcement recorded better energy absorption than pristine BE sample; an increment of 97.30 % impact strength was observed in basalt epoxy composite with graphene nanofiller.

The results indicated that the incorporation of graphene into the fiber, at appropriate proportions, improved the structural performance of basalt/epoxy-graphene composite, rendering it suitable for eco-friendly semi/structural applications. In addition, relevant literature pertaining to this study were thoroughly reviewed, and a comparative summary is presented in Table 4. It was evident that the existing studies differ significantly in several key parameters, including the matrix system, specific surface weight and sourcing of basalt fabrics, graphene type and composite fabrication methodologies. Despite these variations, the current work demonstrated comparatively superior tensile and flexural properties, as achieved through a cost-effective processing route. However, this improvement was not reflected in the impact strength results. This can be attributed to the limited number of fabric layers and the absence of compressive consolidation during fabrication, both effects reduced energy absorption capability. The incorporation of FGO in the present study facilitated uniform dispersion within the epoxy matrix and provided effective secondary reinforcement, thereby contributing to the enhanced mechanical performance observed in both tensile and flexural responses.

4.4. Surface topography analysis of fractured composites by SEM

4.4.1. After tensile test

Fractured surfaces of the composites were subjected to topographic analysis through scanning electron microscopy. SEM images were obtained to understand the basalt-graphene-epoxy bonding mechanisms. Micrographs were taken at different magnifications to explore the nuances between their interactions. Fig. 10(a), (b) and (c) depict the SEM images of tensile fractured samples at three different magnifications: 500 x, 100 kx and 200 kx, respectively. At lowest magnification, the maximum surface area was clearly exposed with different layering arrangement of matrix and fibers or basalt reinforcement. The primary reinforcement of basalt was used as bidirectional woven fabric; therefore, the extension of fibers was observed mutually perpendicular direction after the longitudinal loading. Hence, the linear and lateral arrangements of fibers can take up more load than the unidirectional fiber reinforcement [33]. Furthermore, Fig. 10 (a) shows the cylindrical diameter of fibers in the longitudinal direction and cross line arrangement of fibers in the lateral direction. In the magnified lens, the closely packed fiber-matrix interaction was clearly observed (Fig. 10 b), which supported the enhanced bonding between the polymer/filler mixture and fiber reinforcement. Fig.10 (c) clearly depicts the bending and breakage of fibers, which can be evident from the exposure of uneven circular face at the end. All the images were qualitatively justified the enhanced tensile properties. This can be attributed to better adhesion between the fiber and the graphene-dispersed epoxy, because graphene acted as a nano-interfacial enhancer, improving chemical compatibility, mechanical interlocking and stress transfer between the epoxy and the fiber [34].

Conversely, lack of adhesion between basalt and epoxy was observed from pristine BE composite (sample without graphene). Fig. 11a depicts the loosely dispersed fibers and separated phase of fiber and matrix. In addition, a randomly oriented fibers without any matrix deposition indicated lack of affinity between fiber and matrix, which was observed from the micrograph shown in Fig. 11b. Furthermore, highest magnification image (Fig. 11c) clearly depicts the absence of interlayer between the fibers. The load transfer between the matrix and fiber might have been affected and consequently reduced the load bearing capacity of the composites.

4.4.2. After flexural test

Fig. 12(a)–(c) depict the SEM images taken at the fractured region of the sample after three-point bending test. The combination of tensile and compression effects exhibited the varying magnitude failures in the composites. The alternate layering of matrix and fabric was clearly visible in the lower magnification image, as shown in Fig. 12a. Enriched matrix region (Fig. 12b) surrounding the fiber package exhibited strong bonding between the fiber and matrix and hence, the fiber dislocation was not profound. The presence of interlayer thickness, as shown in Fig. 12c, shows the effective load transfer between fiber and matrix.

Furthermore, a significant amount of fiber breakage was observed, which can be attributed to the compression effect on the fibers from the flexural loading. At the same time, the failure of BE composite (sample without addition of graphene) demonstrated inadequate bonding between the fiber and matrix, as shown in Fig. 13(a)–(c). Loosely separated

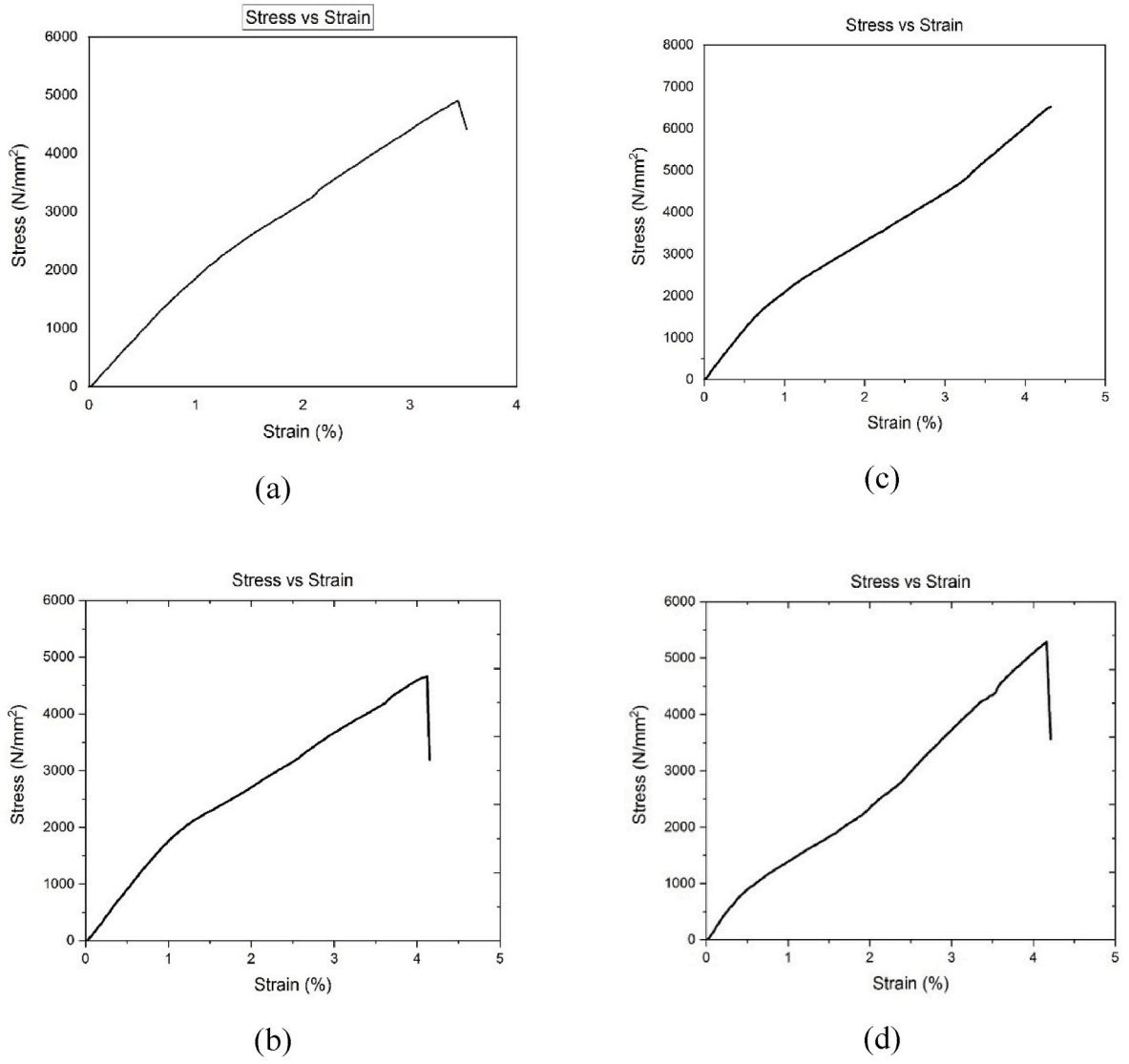

Fig. 7. Stress-strain curves of (a & b) BEG and (c & d) BE samples.

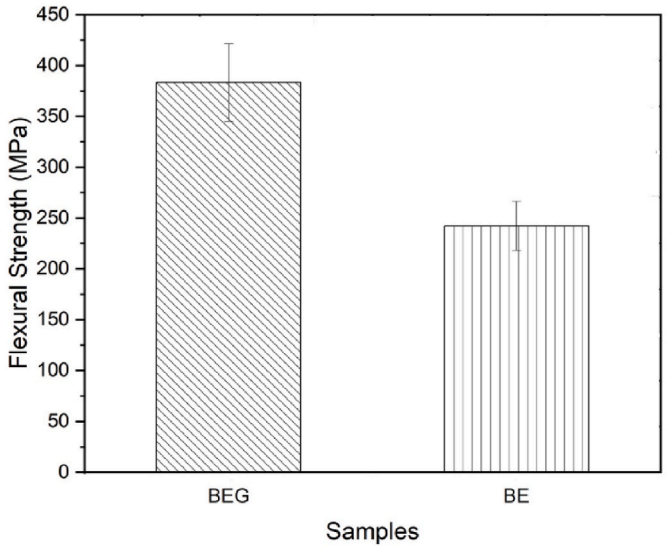

Fig. 8. Flexural strength of the BEG and BE composite samples.

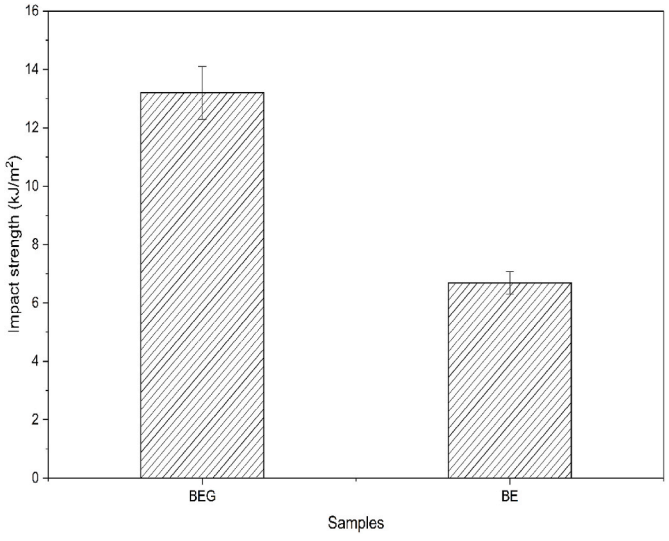

Fig. 9. Impact strengths of the BEG and BE composite samples.

Table 4
Comparative parametric analysis of current research with relevant published works.

Critical parameters	Current work	References	
		[16]	[17]
Matrix	Epoxy LY556 & HY951	Epoxy E−51 + BC126	MGS L285/H285 epoxy
Fiber type & GSM	Basalt plain fabric	Basalt UD	Basalt plain weave
Fiber architecture	Bidirectional	Unidirectional	[0/90] (10 layers)
Specific surface weight (g/m^2)	200	300	200
Type of filler	Reduced graphene oxide	Graphene nanoplates	Graphene nanopellets, possibly more 3D shape
Best filler loading	0.15 wt%	Mechanical: 0.07 wt % Dielectric: 0.24 wt%	Varying filler loading 0.1 wt%, 0.2 wt% and 0.3 wt%
Fabrication method	Solvent dispersion + hand layup	Solvent dispersion + hot press (120 °C)	Hand lay-up + hot press (80 °C)
Tensile strength	216 MPa at 0.15 wt% (↑10 %)	991 MPa at 0.07 % (very high due to UD fabric)	240 MPa at 0.1 wt% (↑13 %)
Flexural strength	383 MPa at 0.15 wt% (↑58 %)	1726 MPa at 0.07 %	273.91 MPa at 0.1 % (↑30 %)
Tensile modulus	2.5 GPa at 0.15 wt% (↑37 %)	44.6 GPa at 0.07 %	15.9 GPa at 0.1 % (↑21 %)
Impact strength	13.2 kJ/m^2 at 0.1 %	Not studied	Peak ≈ 115 kJ/m^2 at 0.1 %
Interfacial adhesion	Rigidly coupled matrix-fiber was observed	Low GNP percolation threshold + interfacial polarization physics	0.1 % improved bonding; agglomeration at higher loadings

fibers were spread across all the fabric layers of the composite (Fig. 13a). The outer layer of the basalt fabric projected its fibers outwards from the matrix, due to the tensile load effect. Both closely packed fibers and significant fiber pullouts were observed (Fig. 13b), which indicated the varying magnitude of loading effect across the thickness of the sample. The clean fiber surface with significant gap between the fibers at the highest magnification established the catastrophic failure at the interface, as observed in Fig. 13c.

4.4.3. After impact test

The fractured composite sample after sudden application of impact load was analyzed through SEM micrographs in Fig. 14(a)–(c). The higher resistance of fiber at the interface led to less fiber pullout and consequently increased the impact strength of the composite. Accordingly, a less amount of fiber pullout was clearly observed in Fig. 14a, which could have led to less energy dissipation. This could happen, due to better bonding between fiber and graphene embedded epoxy matrix. Despite strong interfacial adhesion between fiber and matrix, as observed in Fig. 14b, a substantial fiber sliding occurred by overcoming the frictional resistance at contact surface. A significant amount of matrix surrounded the fiber package (Fig. 14c), reflected the strong adhesion of the matrix to the fiber surface. Closely packed fibers and fiber fracture at the cross-section indicated effective stress transfer, leading to applied stress exceeded the fiber ultimate strength [35].

In the baseline BE composites (sample without graphene in epoxy), excessive fiber pull outs were observed with larger gaps at their interface, as clearly observed in Fig. 15a. Randomly disordered fibers and less amount of matrix deposition on fiber surface were observed (Fig. 15b), which established the insufficient adhesion between fiber and matrix. Fig. 15c with the highest magnified micrograph clearly depicts larger quantity of interfacial gaps between fiber and matrix, and significant

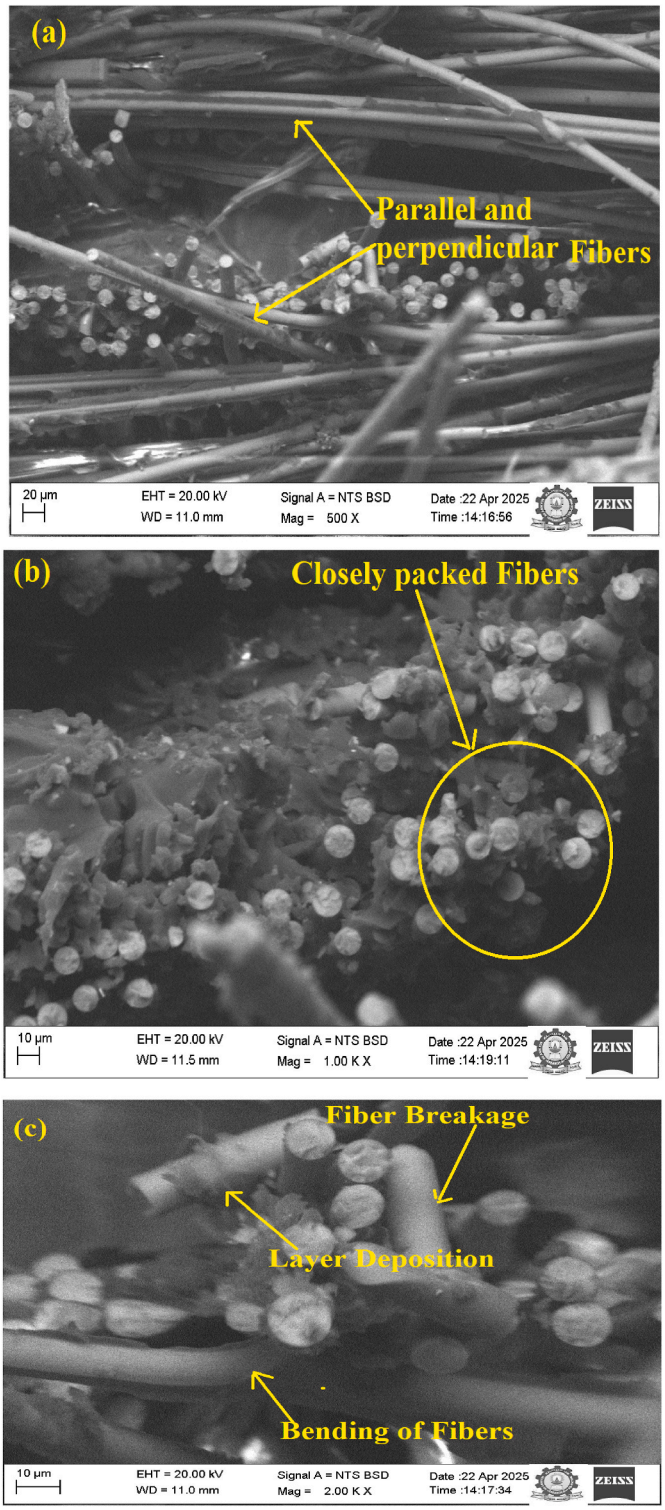

Fig. 10. SEM microstructure of fractured surface of BEG sample after tensile test with different magnifications: (a) 500, (b) 1000 and (c) 2000 x.

number of vacant spots after removal or loss of fibers, due to less frictional resistance at contact surfaces.

5. Dynamic mechanical analysis

Dynamic mechanical analysis (DMA) is a thermo-mechanical characterization technique used to study the viscoelastic behavior of polymers and polymer composites by applying a small oscillatory load as a

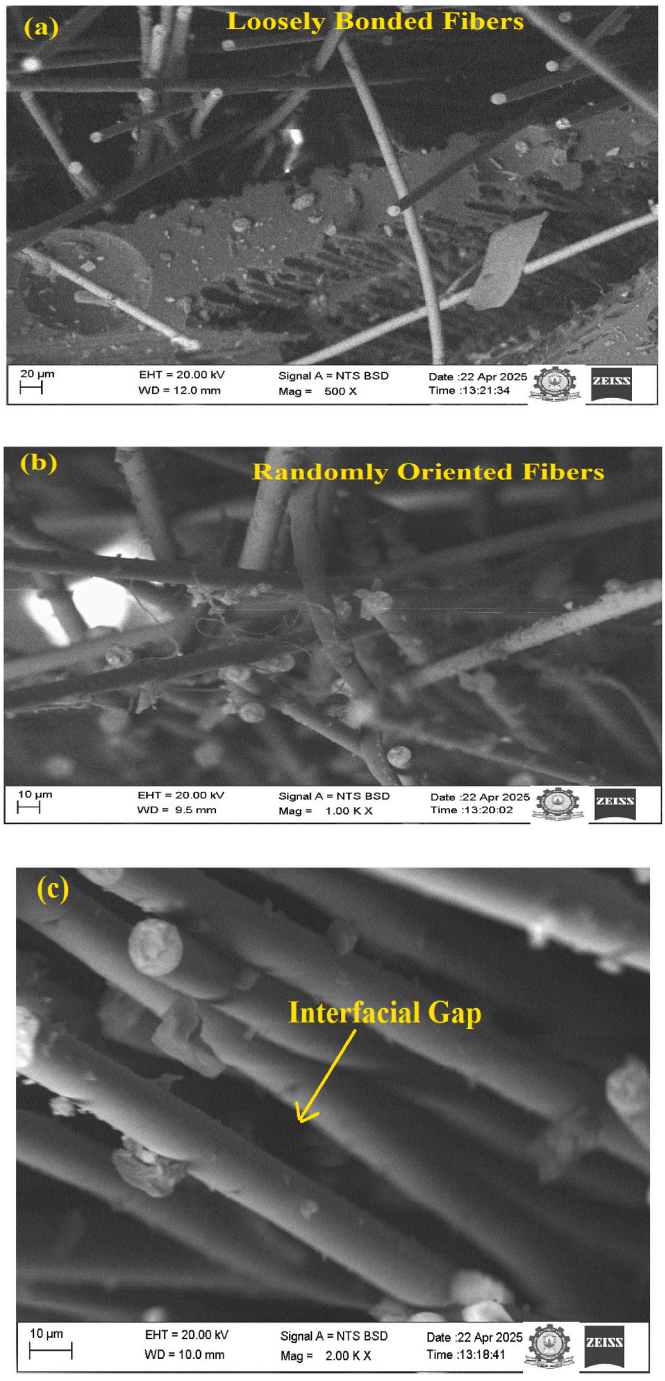

Fig. 11. SEM microstructure of fractured surface of BE sample after tensile test with different magnifications: (a) 500, (b) 1000 and (c) 2000 x.

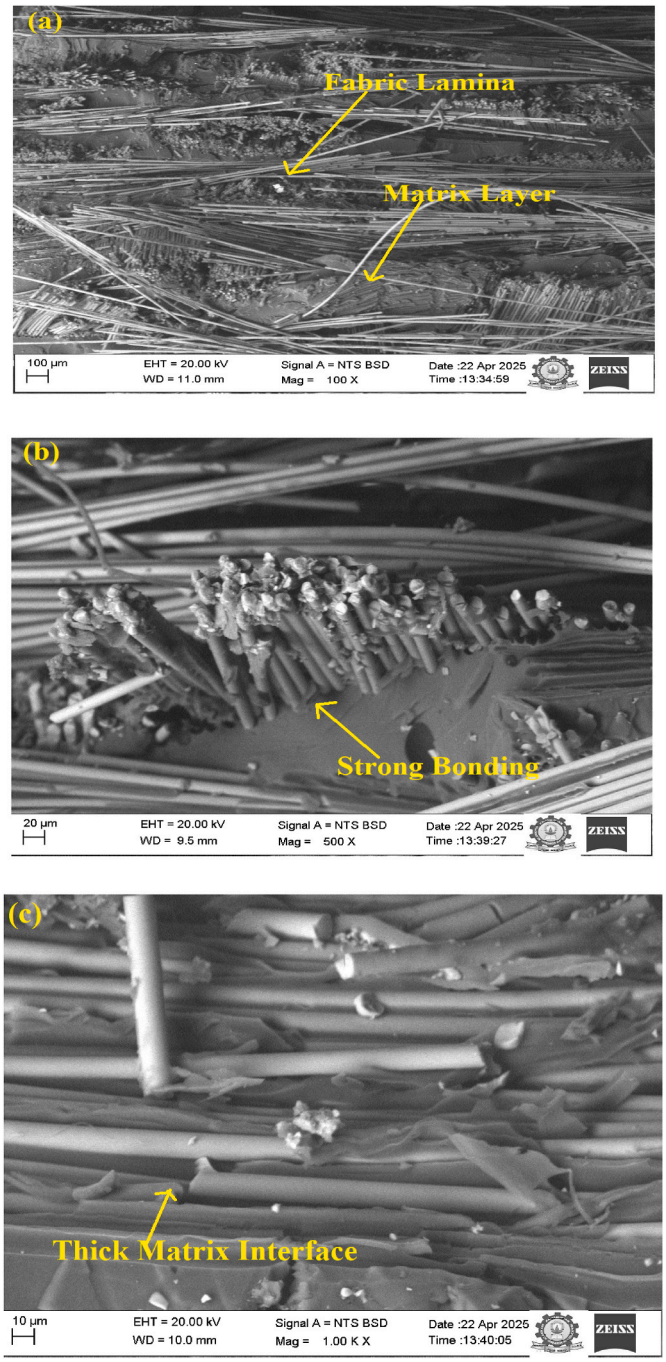

Fig. 12. SEM microstructure of fractured surface of BEG sample after flexural test with different magnifications: (a) 100, (b) 500 and (c) 1000 x.

function of temperature, time or frequency. DMA separates the material response into elastic (energy-storing) and viscous (energy-dissipating) components. Storage, loss moduli and tan delta obtained from DMA provided comprehensive insight into the stiffness, damping behavior, molecular mobility and glass transition characteristics of the samples, as depicted in Fig. 16(a)–(c).

5.1. Storage modulus

Fig. 16a depicts the changes in the storage moduli (E') of the composites as a function of temperature, ranging from 30 to 175 °C. Both samples BEG and BE exhibited a decreasing trend in storage moduli with an increasing temperature. This phenomenon is common to typical polymer-based composites, due to the relaxation of polymer chains within the matrix. A sharp reduction in E′ was observed between 60 and 80 °C, corresponding to the glass transition region, where the material transitioned from a rigid glassy state to a rubbery state.

The graphene induced BFRP showed a maximum storage modulus of approximately 10 GPa, whereas pristine BFRP shows storage modulus of 9 GPa. These improvements can be attributed to GO-assisted interfacial interactions, which strengthen fiber–matrix bonding and improved load transfer, leading to superior mechanical performance.

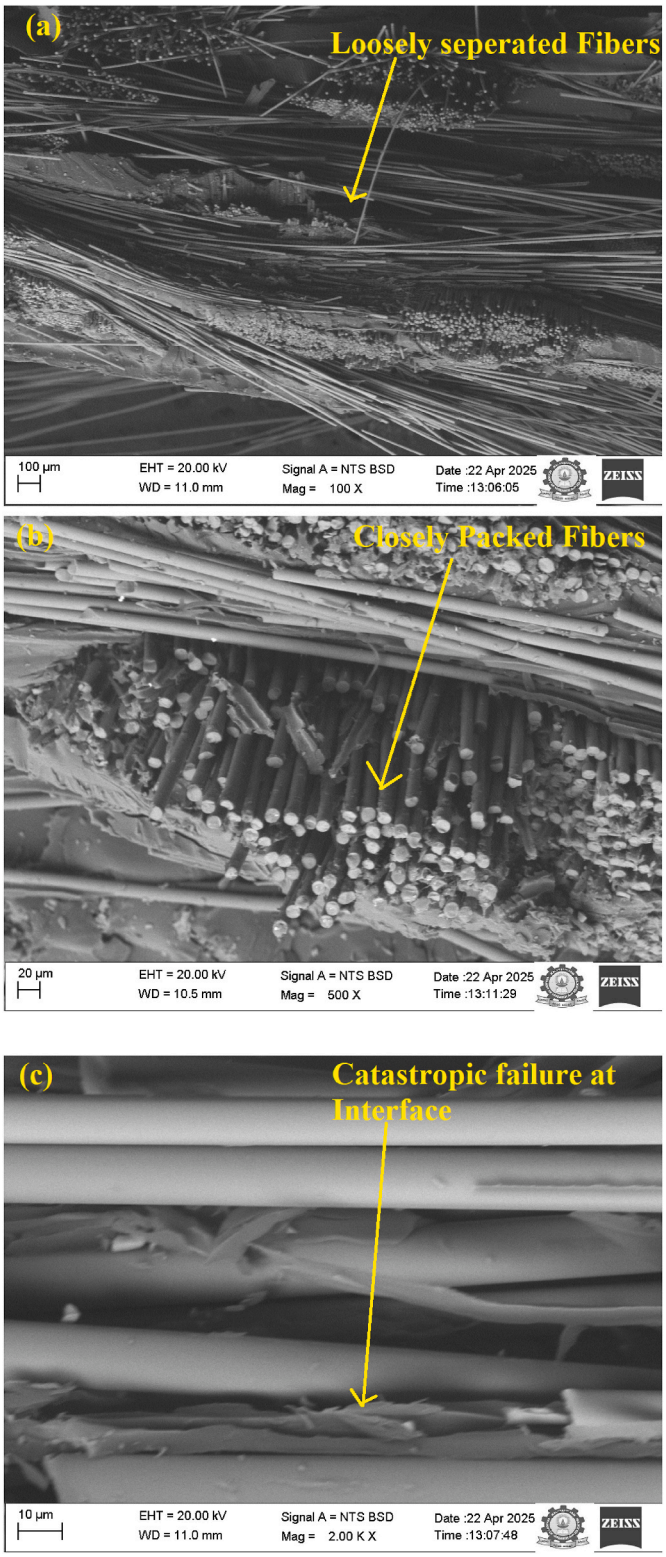

Fig. 13. SEM microstructure of fractured surface of BE sample after flexural test with different magnifications: (a) 100, (b) 500 and (c) 2000 x.

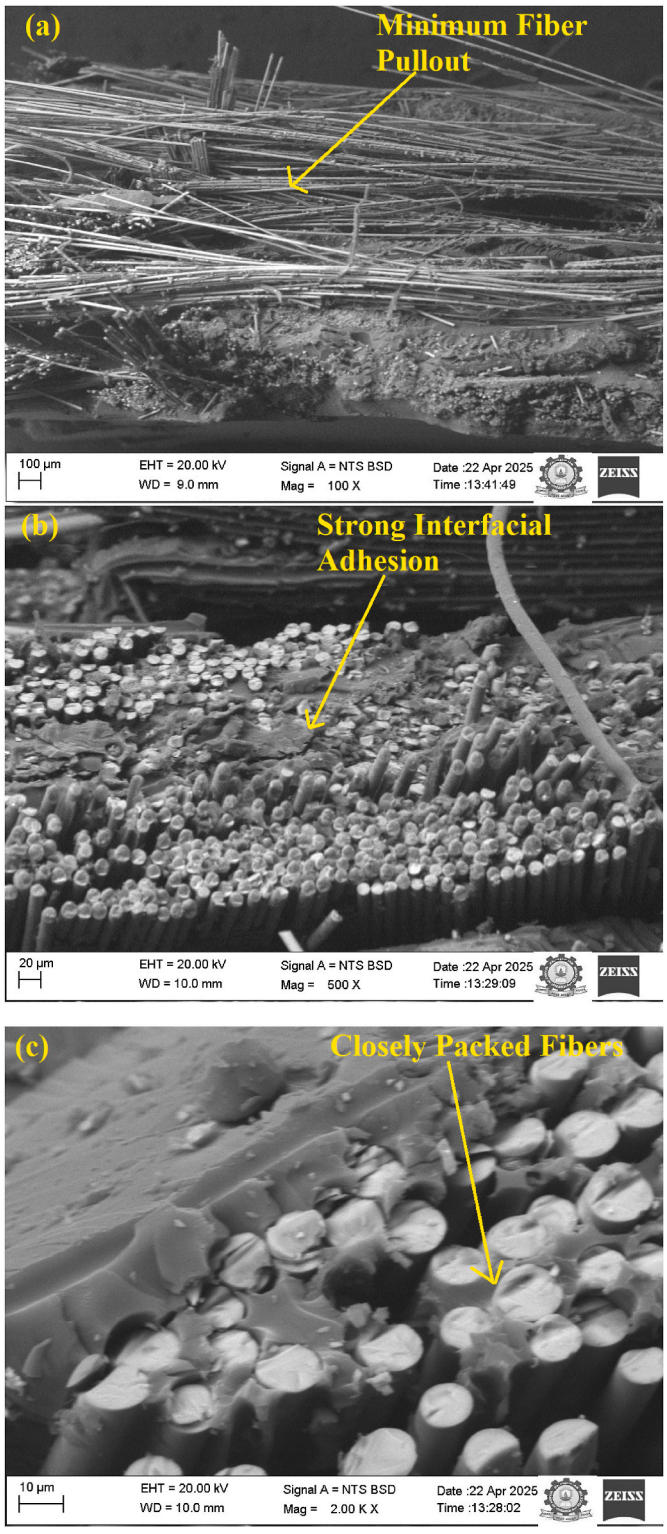

Fig. 14. SEM microstructure of the fractured surface of BEG sample after impact test with different magnifications: (a) 100, (b) 500 and (c) 2000 x.

5.2. Loss modulus

The loss modulus (E″) represents the ability of a material to dissipate mechanical energy and thus reflects its damping behavior. As shown in Fig. 16b, the loss modulus responses of graphene-induced BFRP and pristine BFRP composites differed markedly with temperature, indicating variations in their energy dissipation characteristics. Both composites exhibited a prominent loss modulus peak between 60 and 80 °C, corresponding to the glass transition region of the epoxy matrix. In this temperature range, the polymer underwent a transition from a rigid to a rubbery state, resulting in enhanced molecular motion and increased energy loss. Beyond the peak, the loss modulus decreased as the material entered the rubbery plateau.

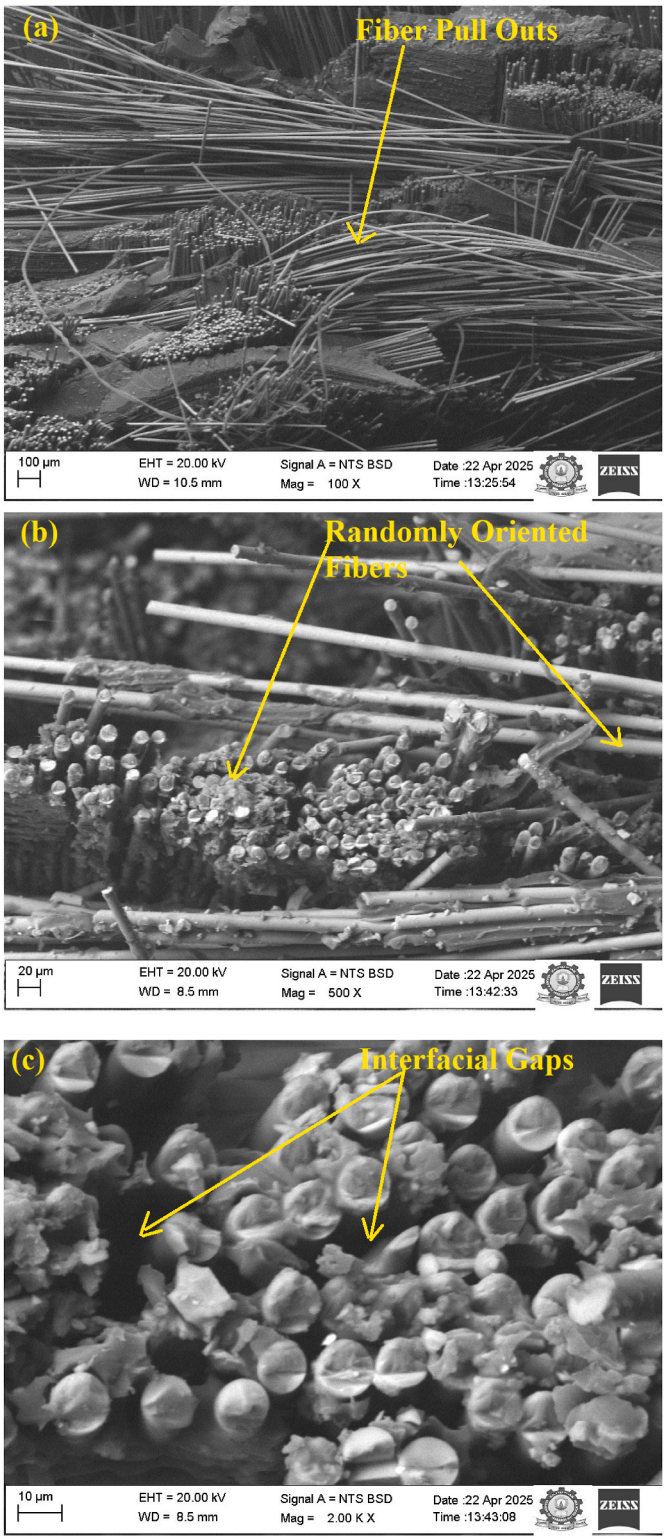

Fig. 15. SEM microstructure of fractured surface of BE sample after impact test with different magnifications: (a) 100, (b) 500 and (c) 2000 x.

The pristine BE composite showed a peak loss modulus of approximately 650 MPa, reflecting moderate damping capability. In contrast, the BEG composites displayed higher peak value when compared with BE at around 680 MPa, indicating improved energy dissipation. This enhancement can be attributed to the addition of graphene, which improved fiber-matrix interfacial interaction, leading to superior damping performance.

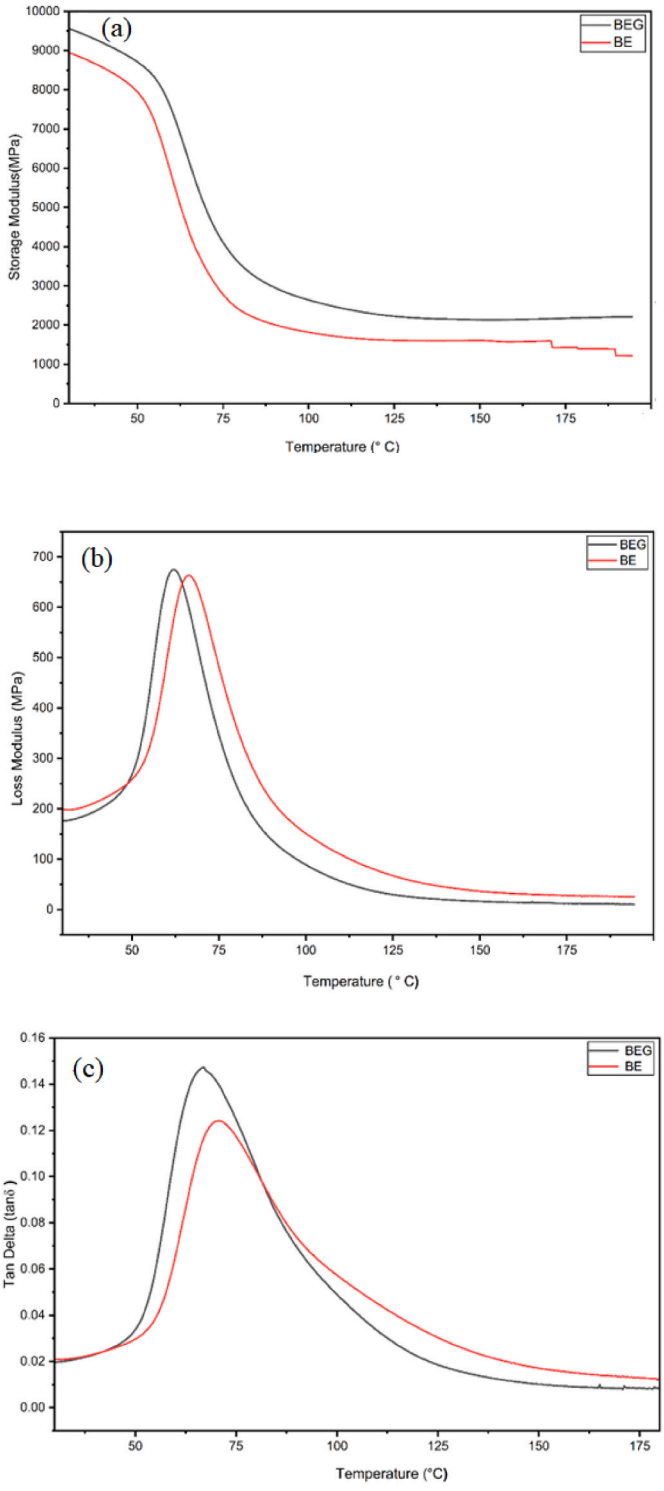

Fig. 16. DMA analysis of pristine (BE) and graphene-induced (BEG) composites, showing their (a) storage, (b) loss moduli and (c) tan delta (tan $^{\delta}$) curves.

5.3. Damping factor

The damping factor (tan δ) provides insight into the energy absorption capability, polymer chain mobility and fiber–matrix interfacial interactions of composite materials. The glass transition temperature (Tg) of the composites is identified from the peak of the tan δ curve, which represents the ratio of loss modulus (E″) to storage modulus (E′) and corresponds to the transition from a rigid glassy state to a flexible rubbery state. As shown in Fig. 16c, BEG and BE composites exhibited

distinct temperature-dependent damping behaviors. For both samples, tan δ increased with temperature and reached a maximum near 70 °C. Beyond this temperature, tan δ decreased as the material entered the rubbery region, where polymer chains required less energy for molecular motion.

The BE composite showed a relatively low tan δ peak, indicating moderate energy dissipation. In contrast, the BEG composite exhibited a higher peak value, suggesting improved damping due to enhanced fiber–matrix interaction and resulting from graphene addition. The graphene-added composite displayed highest tan δ peak, demonstrating superior energy dissipation capability. This improvement can be attributed to the strong interfacial interactions introduced by graphene nanoparticles, which enhanced molecular mobility and structural flexibility. The higher damping factor of the BEG composite highlighted its suitability for applications that require effective energy absorption and impact resistance under dynamic loading conditions, in agreement with previous studies.

6. Thermogravimetric analysis

Thermogravimetric analysis (TGA) wt% curve illustrates the thermal stability and decomposition behavior of a material by showing mass loss as a function of temperature, allowing identification of degradation stages and residual content. Comparing the BEG and BE samples at various temperatures (Fig. 17), it was observed that the uniform weight loss for both occurred up to 450°. Afterwards, BE sample exhibited minimum weight loss when compared with BEG counterpart. Maximum weight loss in graphene-filled materials occurred due to agglomeration, catalytic degradation by graphene defect sites, weak interfacial bonding and decomposition of oxygenated functional groups, which accelerated polymer matrix degradation.

7. Conclusions

Mechanical properties and microstructural behaviors of basalt fiber reinforced epoxy composites with and without graphene as nanofiller, fabricated with hand layup technique have been studied. Microstructural characterizations of the samples were carried out, using SEM. From the results obtained, it was evident that BEG composite sample exhibited better mechanical properties, considering tensile strength and modulus, impact and flexural strengths, as subsequently and briefly inferred.

Considering the studied mechanical properties; 9.98 % increment in tensile strength was observed with BEG composite sample, BEG sample recorded better flexural strength of 58.34 % higher than pristine BE composite sample and impact strength of 97.30 % higher was observed from the BEG composite sample.

Overall, the DMA results confirmed that graphene incorporation significantly enhanced the thermo-mechanical performance of BFRP composites. The BEG samples consistently exhibited higher storage modulus, greater energy dissipation and an elevated damping factor, reflecting improved fiber–matrix interaction and molecular mobility. These enhancements demonstrated the effectiveness of graphene dispersion in strengthening stiffness, dynamic stability and viscoelastic response, thereby making the composite more suitable for applications involving dynamic and thermal loadings.

TGA analysis established that both BEG and BE samples behaved similarly up to 450 °C, but BE composite retained higher thermal stability at elevated temperatures. The increased weight loss in BEG can be associated with graphene agglomeration and defect-induced catalytic degradation, indicating that improved graphene dispersion was essential for enhancing the thermal performance of the composite.

Summarily, it can be deduced that graphene nanofiller played a vital role in enhancement of the mechanical properties of fiber reinforced polymeric composite structure, functioning as a nano-interfacial enhancer and improving chemical compatibility, mechanical interlocking and stress transfer between epoxy and basalt fibers.

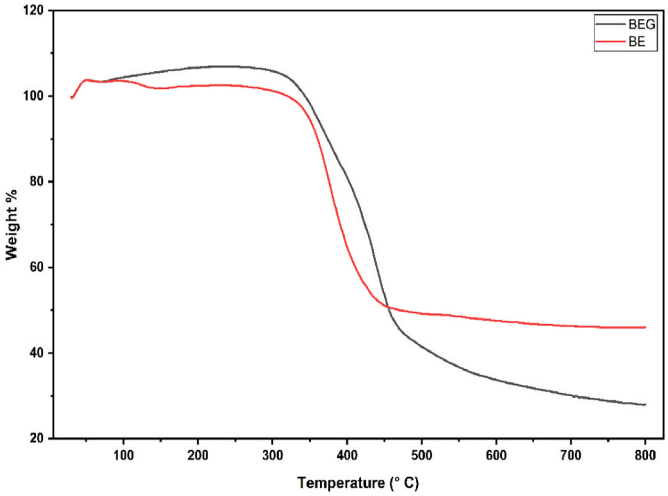

Fig. 17. TGA curves for both composite samples.

Declaration of competing interest

The authors declare that they have no known competing financial interests or personal relationships that could have appeared to influence the work reported in this paper.

Acknowledgement

The authors acknowledge the funding from the Ongoing Research Funding Program (ORF-2025-355), King Saud University, Riyadh, Saudi Arabia.

References

[1] Vaddepalli P, Pankaj K, Rajasri Reddy I. Investigation on mechanical properties and wear behavior of basalt fiber and SiO_2 nanofillers reinforced composites. Results Eng 2024;23:102722. https://doi.org/10.1016/j.rineng.2024.102722.

[2] Manickavasagam Sureshkumar Subburayan, Balachandran Sundaravel, Kim Seong Cheol, Rathinam Balamurugan, Ramkumar Vanaraj. Hybrid epoxy composites reinforced with coconut sheath and basalt fibers: enhancing mechanical and thermal performance for sustainable applications. J Polym Mater/Journal of Polymer Composites 2024. https://doi.org/10.32604/jpm.2024.057901.

[3] Asthana Ankit, Srinivas R, Chauhan Shailendra S, Bandhu Din, Dwivedi Shasi P, Saxena Kuldeep K, Kaur Kirtanjot. Ibrahim alnaser "Development and mechanical properties evaluation of environmentally sustainable composite material using various reinforcements with epoxy.". Case Stud Constr Mater 2024;21:e03624. https://doi.org/10.1016/j.cscm.2024.e03624.

[4] Totaro M, Risitano G, Di Bella G, Crisafulli D, D'Andrea D. A comparative study on mechanical properties and failure mechanisms in basalt and glass fiber reinforced composites. Procedia Struct Integr 2024;66:205–11. https://doi.org/10.1016/j.prostr.2024.11.071.

[5] Mahfuz Kabir Md, Mustak Rubiat, Moinul Hasan Sadik Md. Effect of bio-filler on various properties of glass fiber reinforced epoxy composites. Hybrid Adv 2025;10:100448. https://doi.org/10.1016/j.hybadv.2025.100448.

[6] Prem Anandh A, Sivabalan P, Mohanavel Vinayagam. Thandavamoorthy Raja — Results in Engineering 2025;25. https://doi.org/10.1016/j.rineng.2025.103928. Article 103928.

[7] Velumayil Palanivel's. Hybridization effect on mechanical properties of basalt/kevlar/epoxy composite laminates. Polymers 2022;14(Issue 7). https://doi.org/10.3390/polym14071382.

[8] Shi Xiao-Hui, Luo Huan, Jing Cheng-Yue, Liu Qing-Yun, Wang De-Yi. Effectively enhancing the fire resistance and mechanical properties of basalt fiber/epoxy composites utilizing a novel piperazine phosphonate flame retardant. Constr Build Mater 2025;486. https://doi.org/10.1016/j.conbuildmat.2025.141895. Article 141895.

[9] Palaniyandi Shanmugaselvam, Veeman Dhinakaran. Experimental investigation of mechanical performance of Basalt/Epoxy/MWCNT/SiC reinforced hybrid fiber metal laminates. Mater Res 2022. https://doi.org/10.1590/1980-5373-MR-2022-0174.

[10] Khosravi H., Eslami-Farsani R., "Enhanced mechanical properties of unidirectional basalt fiber/epoxy composites using silane-modified Na^+-montmorillonite nanoclay." DOI: 10.1016/j.polymertesting.2016.08.011.

[11] Wang Q-H, Zhang X-R, Pei X-Q. Study on the friction and wear behavior of basalt fabric composites filled with graphite and nano-SiO_2. Mater Des 2010;31:1403–9. https://doi.org/10.1016/j.matdes.2009.08.041.

[12] Bahari-Sambran F, Eslami-Farsani R, Arbab-Chirani S. The flexural and impact behavior of the laminated aluminum-epoxy/basalt fibers composites containing nanoclay: an experimental investigation. J Sandw Struct Mater 2020;22:1931–51. https://doi.org/10.1177/1099636218792693.
[13] Vinay SS, Sanjay MR, Siengchin S, Venkatesh CV. Effect of Al_2O_3 nanofillers in basalt/epoxy composites: mechanical and tribological properties. Polym Compos 2021;42:1727–40. https://doi.org/10.1002/pc.25927.
[14] Arshad MN, Mohit H, Sanjay MR, Siengchin S, Khan A, Alotaibi MM, Asiri AM, Rub MA. Effect of coir fiber and TiC nanoparticles on basalt fiber reinforced epoxy hybrid composites: physico-mechanical characteristics. Cellulose 2021;28:3451–71. https://doi.org/10.1007/s10570-021-03752-7.
[15] Subagia IA, Tijing LD, Kim Y, Kim CS, Vista FP, Shon HK. (title as indexed). Composites Part B Eng 2014;58:611–7. https://doi.org/10.1016/j.compositesb.2013.10.034.
[16] Chen C, Gu Y, Wang S, Zhang Z, Li M, Zhang Z. Fabrication and characterization of structural/dielectric three-phase composite: continuous basalt fiber-reinforced epoxy resin modified with graphene nanoplates. Compos Appl Sci Manuf 2017;94:199–208. https://doi.org/10.1016/j.compositesa.2016.12.023.
[17] Bulut M. Mechanical characterization of basalt/epoxy composite laminates containing graphene nanopellets. Compos Part B Eng 2017;122:71–8. https://doi.org/10.1016/j.compositesb.2017.04.013.
[18] Lee JH, Rhee KY, Park SJ. The tensile and thermal properties of modified CNT reinforced basalt/epoxy composites. Mater Sci Eng, A 2010;527:6838–43. https://doi.org/10.1016/j.msea.2010.07.080.
[19] Kim M, Lee TW, Park SM, Jeong YG. Structures, electrical and mechanical properties of epoxy composites reinforced with MWCNT-coated basalt fibers. Compos Appl Sci Manuf 2019;123:123–31. https://doi.org/10.1016/j.compositesa.2019.05.011.
[20] Kim MT, Rhee KY, Park SJ, Hui D. Effects of silane-modified carbon nanotubes on flexural and fracture behaviors of carbon nanotube-modified epoxy/basalt composites. Compos Part B: Eng 2012;43:2298–302. https://doi.org/10.1016/j.compositesb.2011.12.007.
[21] Chen W, Shen H, Auad ML, Huang C, Nutt S. Basalt fiber–epoxy laminates with functionalized multi-walled carbon nanotubes. Compos Appl Sci Manuf 2009;40:1082–9. https://doi.org/10.1016/j.compositesa.2009.04.027.
[22] Huanag Xinyankai, et al. Improving the impact resistance of basalt fiber-reinforced polymer composites via a biomimetic nacre structure. Compos Commun 2025;53:102233. https://doi.org/10.1016/j.coco.2024.102233.
[23] Liu Zheng et al. "Effect of seawater corrosion on the mechanical properties of basalt fiber reinforced polymer composites modified by silane coupling agent KH560 and carboxylated carbon nanotubes" Mater Today Commun, doi.org/10.1016/j.mtcomm.2024.109753.
[24] Liu, et al. " Multifunctional basalt fiber reinforced polymer composites with in-situ damage self-sensing and temperature-sensitive behavior". Compos Commun 2024;50:101990. https://doi.org/10.1016/j.coco.2024.101990.
[25] Dong Xiang et al. "Enhanced interfacial interaction, mechanical properties and thermal stability of basalt fiber/epoxy composites with multi-scale reinforcements." https://doi.org/10.1080/09276440.2023.2220500.
[26] [26] Haoming Sun et al."Electrical, mechanical and damage self-sensing properties of basalt fiber reinforced polymer composites modified by electrophoretic deposition" Prog Nat Sci Mater Int .doi.org/10.1016/j.pnsc.2023.11.003.
[27] Park S, et al. Colloidal suspensions of highly reduced graphene oxide in a wide variety of organic solvents. Nano Lett 2009;9(4):1593–7. https://doi.org/10.1021/nl803798y.
[28] Stankovich S, Piner RD, Nguyen SBT, Ruoff RS. Synthesis and exfoliation of isocyanate-treated graphene oxide nanoplatelets. Carbon 2006;44(15):3342–7. https://doi.org/10.1016/j.carbon.2006.06.004.
[29] Ramasundaram S, et al. Increasing hydrophobicity of poly(propylene) fibres by coating reduced graphene oxide and their application as depth filter media. Carbon 2014;70:179–89. https://doi.org/10.1016/j.carbon.2013.12.091.
[30] Sivaranjana P, et al. Enhanced anti corrosion characteristics of epoxy -functionalized graphene oxide nanocomposite coatings on mild steel substrates. J Mater Res Technol 2024;32:3234–45. https://doi.org/10.1016/j-jmrt.2024.08.175.
[31] Muhamad Rusli Halimi, Abdul Razab Mohammad Khairul Azhar, Tajudin Suffian Mohamad, Aziz Mohd Zahri Abdul, Nawi Norazlina Mat, Sulaiman Muhammad Azwadi, Abdullah Reduan, Adam Noraina. Fabrication and evaluation of graphene oxide-enhanced polymer composites for effective radiation shielding in medical applications. Radiat Phys Chem 2026;239:113331. https://doi.org/10.1016/j.radphyschem.2025.113331.
[32] Haoming Sun et al.Failure analysis of glass fiber and basalt fiber reinforced polymer composites under an extreme environment with high-temperature, high-pressure and H2S/CO2 exposure. https://doi.org/10.1002/pc.28462.
[33] Canaroli Lrenzo, Baldi Niccolò, Del Pero Francesco, La Battaglia Vincenzo, Arcidiacono Gabriele, Citti Paolo. Mechanical characterization of carbon fiber composite materials with different reinforcement and thickness cured in autoclave. Hybrid Adv 2025;11:100550. https://doi.org/10.1016/j.hybadv.2025.100550.
[34] Arya Siddhartha, Kumar Ritesh, Chauhan Shakti. Preparation and characterization of woven jute fabric layered composite by using bamboo fiber reinforced polymers as resin matrix. Constr Build Mater 2024;411:134343. https://doi.org/10.1016/j.conbuildmat.2023.134343.
[35] Mohonee VK, Goh KL. Effects of fibre–fibre interaction on stress uptake in discontinuous fibre reinforced composites. Compos B Eng 2016;86:221–8. https://doi.org/10.1016/j.compositesb.2015.10.015.